

Sun-Avoidance Slew Planning Algorithm with Pointing and Actuator Constraints (AAS 19-801)

AIAA/AAS Astrodynamics Specialist Conference,
Portland, ME, 11– 15 August 2019

Mohammad. A. Ayoubi¹ Junette Hsin²

¹Associate Professor, Department of Mechanical Engineering, Santa Clara University,

²Engineer, Dynamics and Control Analysis Group, Maxar Space Infrastructure
(Formerly Space Systems/Loral)

Outlines

- 1 Previous Literature
- 2 Introduction
- 3 Sun-Avoidance Slew (SAS) Algorithm
- 4 Computing Steering Profiles
- 5 Numerical Simulations
- 6 Summary and Conclusion
- 7 Q& A

Introduction

The attitude reorientation problem in the presence of attitude constrained zones has been studied in the last three decades:

- ① McInnes (1994): artificial potential function. He proposed an entirely analytical guidance law which was suitable for onboard implementation.
 - ① However, he used Euler angles, which are singular for large slew angles.
- ② Spindle (1998), Hablani (1998), Biggs and Colley (2016), Frazzoli (2001): A geometric approach was proposed where a feasible attitude maneuver, or a guidance law, is precomputed based on the attitude-avoidance-zone constraints or randomized algorithms.
 - ① However, depending on the number of constraints and initial and final attitudes, this approach can be computationally expensive and not suitable for onboard implementation.

Previous Literature

- 1 Spiller (2016): Particle swarm optimization (PSO) technique to find a sub-optimal solution with keep-out constraints.
- 2 Another approach casted the problem as a convex optimization problem and used semi-definite programming (SDP) or quadratically constrained quadratic programming (QCQP) in its solution (see for instance Kim and Mesbahi, Kim et al., Sun and Dai, and Lee and Mesbahi).
- 3 Recently, Ramos and Schaub proposed a method based on the Lyapunov stability theorem and logarithmic barrier potential function to derive a steering law for attitude control of a spacecraft subject to conically constrained inclusion and exclusion regions. They also considered the control-torque constraint in their algorithm.

SAS Algorithm

- ① The SAS algorithm is a geometric approach for a sun (or any bright object) avoidance slew maneuver with pointing and actuator constraints.
- ② Assumption: spacecraft has a single light-sensitive payload with control-torque and reaction wheels' angular momentum constraints
- ③ Assumption: The initial and final attitudes, instrument boresight vector, and sun vector are known.
- ④ Pontryagin's minimum principle (PMP) is used to derive the desired or target-frame quaternions, angular velocity and acceleration for two cases:
 - ① with control-torque and reaction wheels' angular momentum constraints
 - ② with control-torque constraints
- ⑤ Numerical simulation is performed to show the viability of the proposed algorithm with control-torque and angular momentum constraints.

Sun-Avoidance Slew (SAS) Algorithm

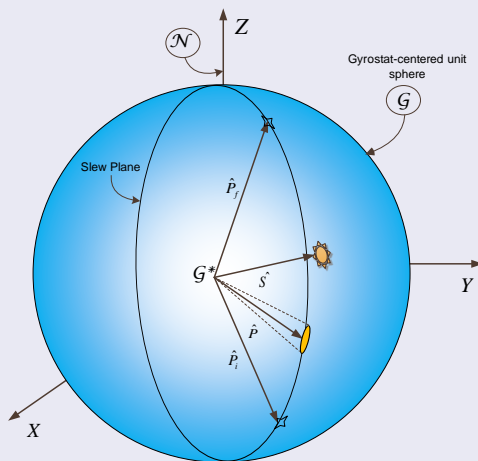


Figure: The gyrostat-centered unit sphere.

Sun-Avoidance Slew (SAS) Algorithm

Problem Statement:

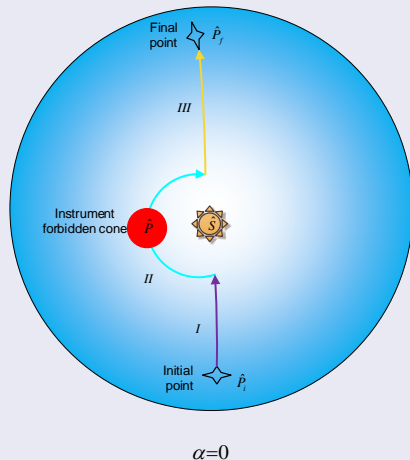
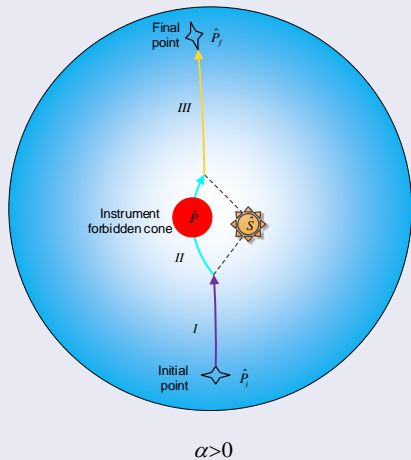
Given: ${}^N\hat{P}_i, {}^N\hat{P}_f, {}^N\hat{S}, {}^g\hat{P}, \epsilon_p, {}^Nq^g, {}^N\omega^g(t_i)$, and ${}^N\omega^g(t_f)$.

Assumption: The spacecraft is rigid.

Find:

- 1 A sequence of slew maneuvers to avoid sun vector.
- 2 the commanded angular velocity, angular acceleration, and quaternion profiles.

Summary of the Algorithm



Sun-Avoidance Slew (SAS) Algorithm

Check the Sun Vector Intrusion

- 1 Check the angular separation, α , between the sun vector, \hat{S} , and the $\hat{P}_i - \hat{P}_f$ or “slew” plane.

$$\alpha = \frac{\pi}{2} - \cos^{-1}(\hat{S} \cdot_{\mathcal{N}} \hat{e}) \quad (1)$$

where the eigenaxis is determined by

$$\hat{e} = \frac{\hat{P}_i \times \hat{P}_f}{|\hat{P}_i \times \hat{P}_f|} \quad (2)$$

- 2 IF $|\alpha| < \epsilon_p$, THEN determine the projection of the sun vector into the slew plane.

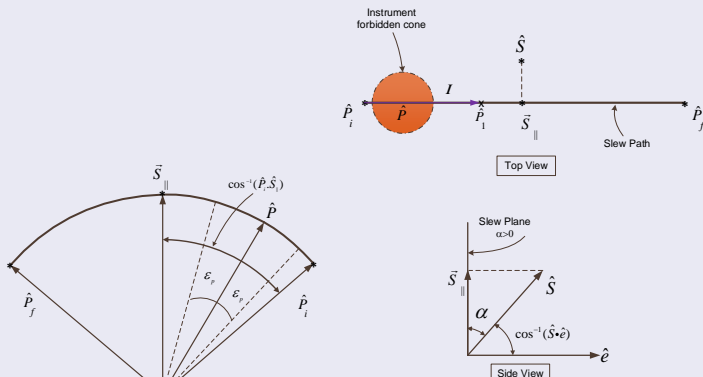
$$\vec{S}_{||} = \hat{S} \cos \alpha \quad (3)$$

Sun-Avoidance Slew (SAS) Algorithm

Slew Maneuvers

① The 1st slew around the eigenaxis, \hat{e} , through angle:

$$\phi_1 = \begin{cases} \cos^{-1}(\hat{P}_i \cdot_G \hat{S}_{||}) - \epsilon_p & \text{when } \cos^{-1}(\hat{P}_i \cdot_G \hat{S}_{||}) - \epsilon_p \leq \pi \\ \cos^{-1}(\hat{P}_i \cdot_G \hat{S}_{||}) - \epsilon_p - 2\pi & \text{when } \cos^{-1}(\hat{P}_i \cdot_G \hat{S}_{||}) - \epsilon_p > \pi \end{cases} \quad (4)$$

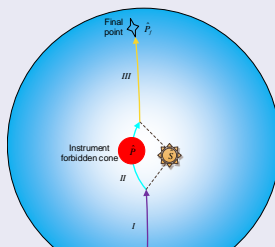
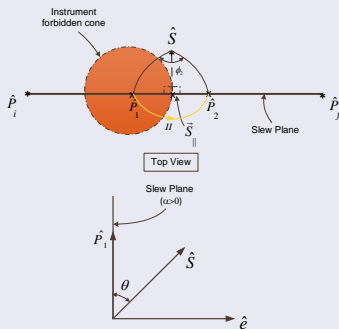


Sun-Avoidance Slew (SAS) Algorithm

Slew Maneuvers

- 2 The 2nd slew around the unit sun vector, \hat{S} , via ϕ_2 .
 when $\alpha \neq 0$

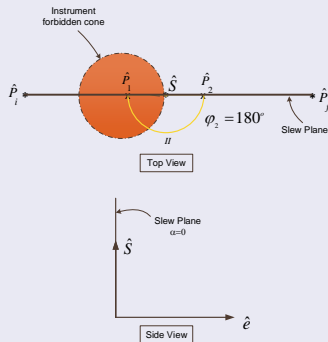
$$\phi_2 = 2 \tan^{-1} \left[\frac{\hat{S} \cdot (\hat{P}_1 \times \hat{S}_{||})}{(\hat{P}_1 \cdot \hat{S}_{||}) - (\hat{S} \cdot \hat{P}_1)(\hat{S} \cdot \hat{S}_{||})} \right], \quad (5)$$



Sun-Avoidance Slew (SAS) Algorithm

Slew Maneuvers

- 2 The 2nd slew around the unit sun vector, \hat{S} , via $\phi_2 = 180^\circ$.
b) when $\alpha = 0$

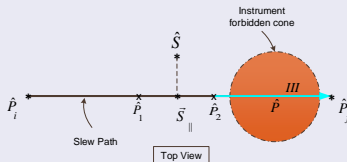
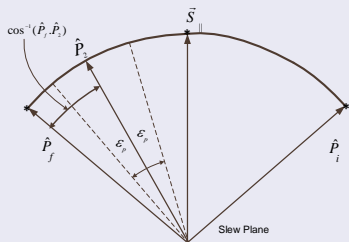


Sun-Avoidance Slew (SAS) Algorithm

Slew Maneuvers

- 3 The 3rd slew about the \hat{e} through angle:

$$\phi_3 = \begin{cases} \cos^{-1}({}_G\hat{P}_f \cdot \hat{P}_2) & \text{when } {}_G\hat{P}_f \cdot \hat{P}_2 \geq 0 \\ \cos^{-1}({}_G\hat{P}_f \cdot \hat{P}_2) - 2\pi & \text{when } {}_G\hat{P}_f \cdot \hat{P}_2 < 0 \end{cases} \quad (6)$$



- 4 The final slew is about the instrument boresight axis to go to the final attitude.

Summary of the Algorithm

- 1 Slew around the eigenaxis, \hat{e} , through angle:

$$\phi_1 = \begin{cases} \cos^{-1}(\hat{P}_i \cdot_G \hat{S}_{||}) - \epsilon_p & \text{when } \cos^{-1}(\hat{P}_i \cdot_G \hat{S}_{||}) - \epsilon_p \leq \pi \\ \cos^{-1}(\hat{P}_i \cdot_G \hat{S}_{||}) - \epsilon_p - 2\pi & \text{when } \cos^{-1}(\hat{P}_i \cdot_G \hat{S}_{||}) - \epsilon_p > \pi \end{cases} \quad (7)$$

- 2 Slew around the \hat{S} via:

$$\phi_2 = \begin{cases} \phi_2 = 2 \tan^{-1} \left[\frac{\hat{S} \cdot (\hat{P}_1 \times \hat{S}_{||})}{(\hat{P}_1 \cdot \hat{S}_{||}) - (\hat{S} \cdot \hat{P}_1)(\hat{S} \cdot \hat{S}_{||})} \right], & \text{when } \alpha \neq 0 \\ \pi & \text{when } \alpha = 0 \end{cases} \quad (8)$$

- 3 Slew about the \hat{e} through angle:

$$\phi_3 = \begin{cases} \cos^{-1}({}_G \hat{P}_f \cdot \hat{P}_2) & \text{when } {}_G \hat{P}_f \cdot \hat{P}_2 \geq 0 \\ \cos^{-1}({}_G \hat{P}_f \cdot \hat{P}_2) - 2\pi & \text{when } {}_G \hat{P}_f \cdot \hat{P}_2 < 0 \end{cases} \quad (9)$$

Computing the Steering Profiles

Single-Axis, Agile Slew Maneuver with Velocity and Acceleration Constraints.

Computing Steering Profiles

Problem Statement

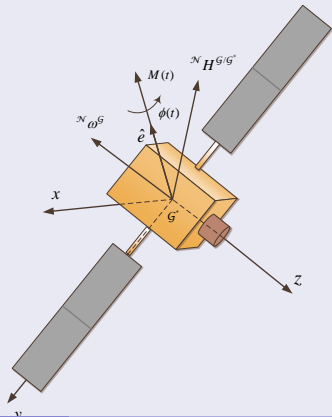
Consider the motion of a **rigid** spacecraft around a given inertially-fixed axis, ${}^G\hat{e} = [e_x, e_y, e_z]^T$. The problem of minimum-time slew maneuver around the \hat{e} axis can be formulated as

$$\underset{u}{\text{Minimize}} J[x(.), u(.), t_f] = \int_{t_0}^{t_f} dt, \quad (10)$$

subject to the following dynamic constraint

$$\Sigma : \begin{cases} \dot{x}_1 = x_2, \\ \dot{x}_2 = M/I_{\hat{e}}^{G/G^*} = u, \end{cases} \quad (11)$$

where $x_1 \triangleq \phi$ and $x_2 = \dot{\phi}$.



Computing Steering Profiles

Problem Statement Continued

The boundary conditions are

$$BCs : \begin{cases} \phi(t_0) = 0, \phi(t_f) = \phi_f, \\ \dot{\phi}(t_0) = \dot{\phi}_0, \dot{\phi}(t_f) = \dot{\phi}_f, \end{cases} \quad (12)$$

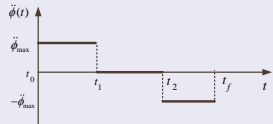
and velocity (state) and acceleration (control) constraints are

$$C_1 : \begin{cases} |x_2 = \dot{\phi}| \leq \dot{\phi}_{max}, \\ |u = \ddot{\phi}| \leq \ddot{\phi}_{max}, \end{cases} \quad (13)$$

Find: $\phi(t)$, $\dot{\phi}(t)$, and $\ddot{\phi}(t)$.

Computing Steering Profiles

- Angular acceleration profile (bang-off-bang):

$$\ddot{\phi}(t) = u = \begin{cases} \ddot{\phi}_{max} & \text{when } t_0 \leq t \leq t_1, \\ 0 & \text{when } t_1 \leq t \leq t_2, \\ -\ddot{\phi}_{max} & \text{when } t_2 \leq t \leq t_f. \end{cases} \quad (14)$$


- Angular velocity profile:

$$\dot{\phi}(t) = \begin{cases} \dot{\phi}_0 + \ddot{\phi}_{max}(t - t_0) & \text{when } t_0 \leq t \leq t_1, \\ \dot{\phi}_{max} & \text{when } t_1 \leq t \leq t_2, \\ \dot{\phi}_{max} - \ddot{\phi}_{max}(t - t_2) & \text{when } t_2 \leq t \leq t_f. \end{cases} \quad (15)$$

- Angular position profile:

$$\phi(t) = \begin{cases} \dot{\phi}_0(t - t_0) + \frac{1}{2}\ddot{\phi}_{max}(t - t_0)^2 & \text{when } t_0 \leq t \leq t_1, \\ \phi(t_1) + \dot{\phi}_{max}(t - t_1) & \text{when } t_1 \leq t \leq t_2, \\ \phi(t_2) + \dot{\phi}_{max}(t - t_2) - \frac{1}{2}\ddot{\phi}_{max}(t - t_2)^2 & \text{when } t_2 \leq t \leq t_f. \end{cases} \quad (16)$$

Computing Steering Profiles

- Using the conditions, $\dot{\phi}(t_1) = \dot{\phi}_{max}$, $\dot{\phi}(t_f) = \dot{\phi}_f$, $\phi(t_f) = \phi_f$, we can determine switching times t_1 , t_2 , and final time t_f as:

$$t_1 = t_0 + \frac{\dot{\phi}_{max} - \dot{\phi}_0}{\ddot{\phi}_{max}}, \quad (17)$$

$$t_2 = t_1 + \frac{1}{\dot{\phi}_{max}} \left[\phi_f - \dot{\phi}_0(t_1 - t_0) - \frac{1}{2} \ddot{\phi}_{max}(t_1 - t_0)^2 - \frac{\dot{\phi}_{max}(\dot{\phi}_{max} - \dot{\phi}_f)}{\ddot{\phi}_{max}} + \frac{(\dot{\phi}_{max} - \dot{\phi}_f)^2}{2\ddot{\phi}_{max}} \right], \quad (18)$$

and

$$t_f = t_1 + \frac{1}{\dot{\phi}_{max}} \left[\phi_f - \dot{\phi}_0(t_1 - t_0) - \frac{1}{2} \ddot{\phi}_{max}(t_1 - t_0)^2 + \frac{(\dot{\phi}_{max} - \dot{\phi}_f)^2}{2\ddot{\phi}_{max}} \right]. \quad (19)$$

Computing Steering Profiles

- Steering profiles:

$${}^Nq^D(t) = [e_x \sin \frac{\phi(t)}{2}, e_y \sin \frac{\phi(t)}{2}, e_z \sin \frac{\phi(t)}{2}, \cos \frac{\phi(t)}{2}]^T \quad (20)$$

$${}^N_G\omega^D(t) = \dot{\phi}(t)_G \hat{e} \quad (21)$$

$${}^N_G\alpha^D(t) = \ddot{\phi}(t)_G \hat{e} \quad (22)$$

Numerical Simulations

Introduction

- 1 Matlab was used to numerically simulate and examine the proposed algorithm.
- 2 The initial, final, and sun position vectors were randomized for each run.
- 3 Two cases shown in these slides - one in which the sun angle is greater than 0 from the slew plane, the other in which the sun vector lies directly on the slew plane.
- 4 Slew angles were found using the methods discussed in the description of the algorithm.

Numerical Simulations

$$\alpha > 0$$

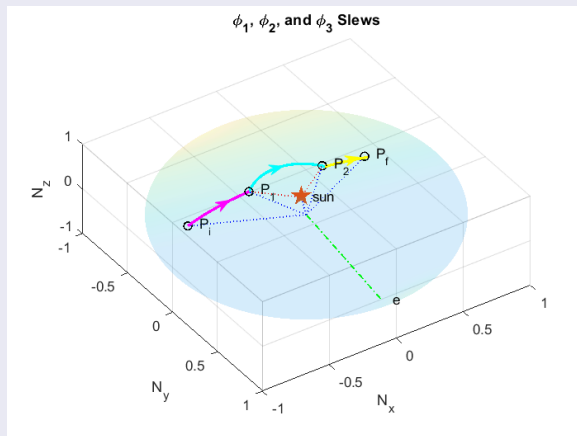


Figure: Attitude Profile of the Entire Slew

Numerical Simulations

$\alpha \dot{\omega}$

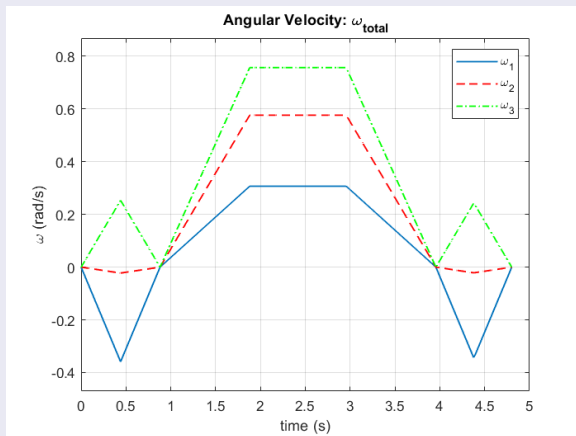


Figure: Angular Velocity in Spacecraft Frame

Numerical Simulations

$$\alpha > 0$$

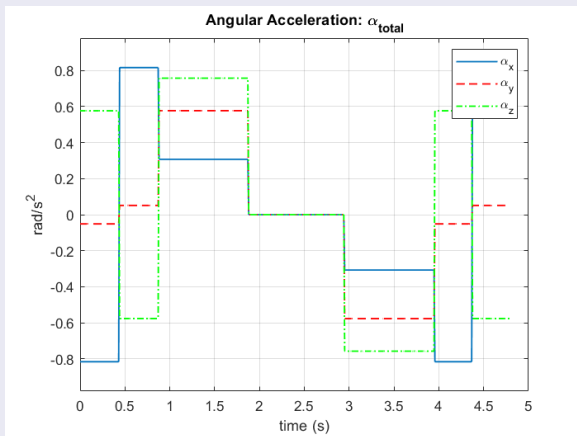


Figure: Angular Acceleration

Numerical Simulations

$$\alpha > 0$$

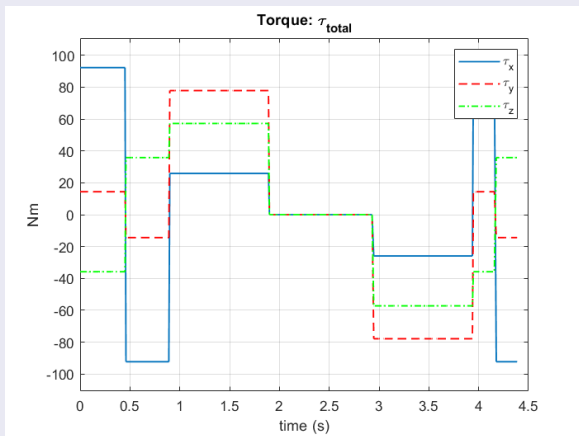


Figure: Torque Applied from Actuator System

Numerical Simulations

$$\alpha > 0$$

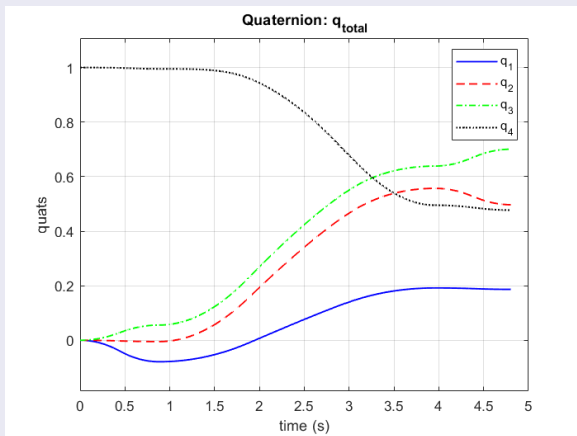


Figure: Quaternion Attitude

Summary and Conclusion

- 1 Geometric approach for large-angle slew planning with pointing and actuator constraints
- 2 Assumed that initial and final attitudes, instrument boresight, and sun vector are known
- 3 Target-frame quaternions, angular velocities, and angular accelerations are derived base on the PMP
- 4 Limitation is for single sensitive-payload

Acknowledgments

The research has been supported by Maxar Space Solutions (formerly Space Systems/Loral). The second author (Junette Hsin) would like to acknowledge Luke DeGalan for his useful comments.

Q & A

Back-up Slides

Computing the Steering Profiles

Case II: Single-Axis, Agile Slew Maneuver with Acceleration Constraint.

Single-Axis, Agile Slew Maneuver with Acceleration Constraint

Problem Statement:

Consider the optimal control problem described by Eqs.(10), (11), (12), and subject to control constraint

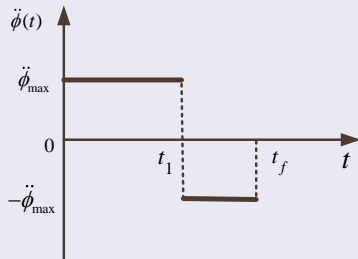
$$C_2 : |u = \ddot{\phi}| \leq \ddot{\phi}_{max}. \quad (23)$$

Find: $\phi(t)$, $\dot{\phi}(t)$, and $\ddot{\phi}(t)$.

Single-Axis, Agile Slew Maneuver with Acceleration Constraint

- Angular acceleration about the \hat{e} axis:

$$\ddot{\phi}(t) = \ddot{\phi}_{\max} \mathbb{U}(t_0) - 2\ddot{\phi}_{\max} \mathbb{U}(t - t_1) \quad (24)$$



where the switching and the final times are given by

$$t_1 = t_0 - \frac{\dot{\phi}_0}{\ddot{\phi}_{\max}} + \frac{\sqrt{\ddot{\phi}_{\max}^2(2\ddot{\phi}_{\max}\phi_f + \dot{\phi}_f^2 + \dot{\phi}_0^2)}}{\sqrt{2}\ddot{\phi}_{\max}^2} \quad (25)$$

Single-Axis, Agile Slew Maneuver with Acceleration Constraint

and

$$t_f = t_0 - \frac{\dot{\phi}_f + \dot{\phi}_0}{\ddot{\phi}_{max}} + \frac{\sqrt{2}\sqrt{\ddot{\phi}_{max}^2(2\ddot{\phi}_{max}\phi_f + \dot{\phi}_{ef}^2 + \dot{\phi}_0^2)}}{\ddot{\phi}_{max}^2} \quad (26)$$

- Angular velocity about the \hat{e} axis:

$$\dot{\phi}(t) = \dot{\phi}_0 + \ddot{\phi}_{max}(t - t_0)\mathbb{U}(t_0) - 2\ddot{\phi}_{max}(t - t_1)\mathbb{U}(t - t_1) \quad (27)$$

- Angular position about the \hat{e} axis:

$$\begin{aligned} \phi(t) = & \dot{\phi}_0(t - t_0) + \ddot{\phi}_{max}\frac{(t - t_0)^2}{2}\mathbb{U}(t_0) \\ & - 2\ddot{\phi}_{max}\frac{(t - t_1)^2}{2}\mathbb{U}(t - t_1) \end{aligned} \quad (28)$$

The Agile Sun-Avoidance Slew Maneuver

The First Slew Maneuver:

A single-axis nonrest-to-rest maneuver around the \hat{e}

- The BCs:

$$\dot{\phi}(t_0) = \dot{\phi}_0, \phi(t_0) = 0, \dot{\phi}(t_{f1}) = 0, \phi(t_{f1}) = \phi_1. \quad (29)$$

The switching time, t_{11} , and minimum-time, t_{f1} , are

$$t_{11} = t_0 - \frac{\dot{\phi}_0}{\ddot{\phi}_{max}} + \frac{\sqrt{\ddot{\phi}_{max}^2(2\ddot{\phi}_{max}\phi_1 + \dot{\phi}_0^2)}}{\sqrt{2}\ddot{\phi}_{max}^2} \quad (30)$$

$$t_{f1} = t_0 - \frac{\dot{\phi}_0}{\ddot{\phi}_{max}} + \frac{\sqrt{2\ddot{\phi}_{max}^2(2\ddot{\phi}_{max}\phi_1 + \dot{\phi}_0^2)}}{\ddot{\phi}_{max}^2} \quad (31)$$

The $\ddot{\phi}(t)$, $\dot{\phi}(t)$, and $\phi(t)$, can be found by substituting the boundary conditions given by (29) and t_{11} and t_{f1} in to Eqs. (24), (27), and (28), respectively.

The Agile Sun-Avoidance Slew Maneuver

The Second Slew Maneuver: A rest-to-rest maneuver around the sun vector

- The BCs:

$$\dot{\phi}(t_0) = 0, \phi(t_0) = 0, \dot{\phi}(t_{f2}) = 0, \phi(t_{f2}) = \phi_2. \quad (32)$$

The switching time, t_{12} , and the minimum-time, t_{f2} , are

$$t_{12} = t_0 - \frac{\sqrt{\phi_2}}{\ddot{\phi}_{max}} \quad (33)$$

$$t_{f2} = t_0 - \frac{2\sqrt{\phi_2}}{\ddot{\phi}_{max}} \quad (34)$$

The $\ddot{\phi}(t)$, $\dot{\phi}(t)$, and $\phi(t)$, can be found by substituting the boundary conditions given by (32) and t_{12} and t_{f2} in to Eqs. (24), (27), and (28), respectively.

The Agile Sun-Avoidance Slew Maneuver

The Third Slew Maneuver: A single-axis rest-to-nonrest maneuver around the \hat{e}

- The BCs:

$$\dot{\phi}(t_0) = 0, \phi(t_0) = 0, \dot{\phi}(t_{f3}) = \dot{\phi}_f, \phi(t_{f3}) = \phi_3. \quad (35)$$

The switching time, t_{13} , and the minimum-time, t_{f3} , are

$$t_{13} = t_0 + \frac{\sqrt{\ddot{\phi}_{max}^2(2\ddot{\phi}_{max}\phi_3 + \dot{\phi}_f^2)}}{\sqrt{2}\ddot{\phi}_{max}^2} \quad (36)$$

$$t_{f3} = t_0 - \frac{\dot{\phi}_f}{\ddot{\phi}_{max}} + \frac{\sqrt{2\ddot{\phi}_{max}^2(2\ddot{\phi}_{max}\phi_3 + \dot{\phi}_f^2)}}{\ddot{\phi}_{max}^2} \quad (37)$$

The $\ddot{\phi}(t)$, $\dot{\phi}(t)$, and $\phi(t)$, can be found by substituting the boundary conditions given by (35) and t_{13} and t_{f3} in to Eqs. (24), (27), and (28), respectively.

Computing Steering Profiles

Using the Pontryagin's minimum principle (PMP), we derive the necessary conditions for the optimal solution as follows:

① State Eqs.:

$$\begin{cases} \dot{x}_1 = x_2, \\ \dot{x}_2 = u, \\ \dot{x}_3 = (x_2 + \dot{\phi}_{max})^2 \mathbb{U}(-x_2 - \dot{\phi}_{max}) + (\dot{\phi}_{max} - x_2)^2 \mathbb{U}(x_2 - \dot{\phi}_{max}), \end{cases} \quad (38)$$

where the unit step function, \mathbb{U} , is defined as

$$\mathbb{U}(X) = \begin{cases} 1, X > 0, \\ 0, X \leq 0. \end{cases} \quad (39)$$

Note: $(x_3(t_0) = x_3(t_f) = 0 \ \& \ x_3(t) \geq 0) \rightarrow x_3(t) = 0, \forall t \in [t_0, t_f]$.

② Hamiltonian:

$$\begin{aligned} \mathcal{H} = & 1 + \lambda_1 x_2 + \lambda_2 u + \lambda_3 \left[(x_2 + \dot{\phi}_{max})^2 \mathbb{U}(-x_2 - \dot{\phi}_{max}) \right. \\ & \left. (\dot{\phi}_{max} - x_2)^2 \mathbb{U}(x_2 - \dot{\phi}_{max}) \right] \end{aligned} \quad (40)$$

Computing Steering Profiles

3 Costate Eqs.:

$$\begin{cases} \dot{\lambda}_1 = -\frac{\partial \mathcal{H}}{\partial x_1} = 0, \\ \dot{\lambda}_2 = -\frac{\partial \mathcal{H}}{\partial x_2} = -\lambda_1 - 2\lambda_3(x_2 + \dot{\phi}_{max})\mathbb{U}(-x_2 - \dot{\phi}_{max}) \\ \quad + 2\lambda_3(\dot{\phi}_{max} - x_2)\mathbb{U}(x_2 - \dot{\phi}_{max}), \\ \dot{\lambda}_3 = -\frac{\partial \mathcal{H}}{\partial x_3} = 0. \end{cases} \quad (41)$$

4 Applying the Pontryagin's minimum principle (PMP),

$$u^* = \underset{u \in \mathcal{U}}{\operatorname{argmin}} \mathcal{H}, \quad (42)$$

where \mathcal{U} defines the domain of feasible controls. The optimal control can be determined as

$$u^*(t) = \begin{cases} \ddot{\phi}_{max} \lambda_2 < 0, \\ \quad ? \lambda_2 = 0, \\ -\ddot{\phi}_{max} \lambda_2 > 0. \end{cases} \quad (43)$$

This is a *singular arc* optimal control problem.

Computing Steering Profiles

- 5 Determining the optimal control in the singular arc:

$$\frac{d^2}{dt^2} \left(\frac{\partial \mathcal{H}}{\partial u} \right) = \ddot{\lambda}_2 = 0 \rightarrow \dot{x}_2 = 0 \rightarrow u^* = 0 \quad (44)$$

- 6 Checking the Generalized Legendre-Clebsch condition for optimality:

$$(-1)^2 \frac{\partial}{\partial u} \left[\frac{d^2}{dt^2} \left(\frac{\partial \mathcal{H}}{\partial u} \right) \right] = 1 \geq 0 \quad (45)$$

- 7 The transversality condition:

$$\mathcal{H}|_{(*, t_f)} = 0 \text{ and } \mathcal{H} \neq \mathcal{H}(t) \rightarrow \mathcal{H} = 0, \forall t \in [t_0, t_f]. \quad (46)$$

Numerical Simulations

$$\alpha = 0$$

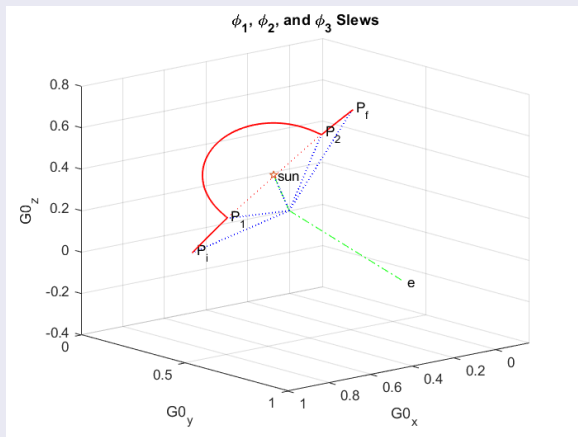


Figure: Attitude Profile of the Entire Slew

Numerical Simulations

$$\alpha = 0$$

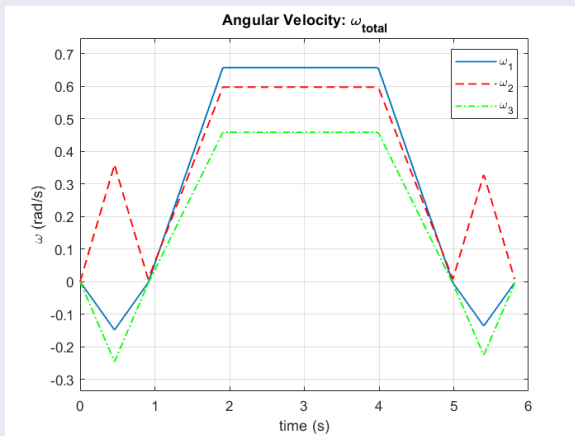


Figure: Angular Velocity in Spacecraft Frame

Numerical Simulations

$$\alpha = 0$$

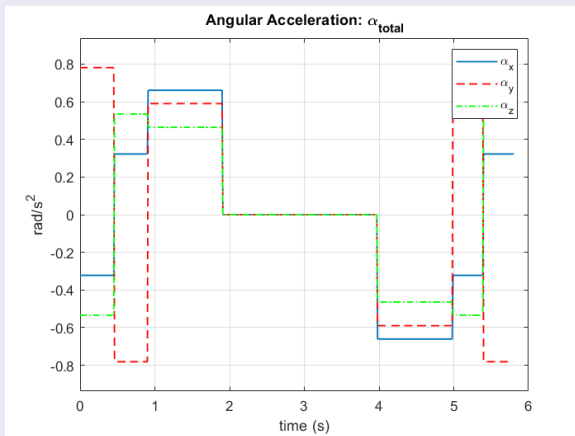


Figure: Angular Acceleration

Numerical Simulations

$$\alpha = 0$$

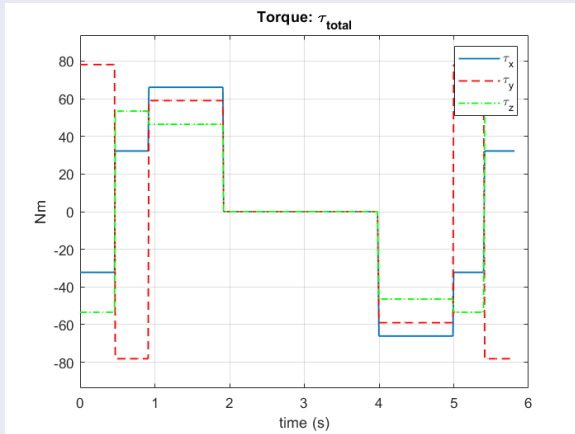


Figure: Torque Applied from Actuator System

Numerical Simulations

$$\alpha = 0$$

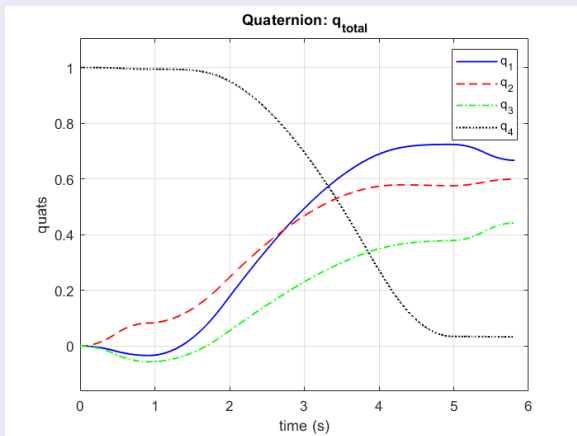


Figure: Quaternion Attitude